

BNL-99426-2013-TECH C-A/AP/276;BNL-99426-2013-IR

Modeling RHIC Linear Chromaticity with Sextupole Components in the Arc Main Dipoles

Y. Luo

May 2007

Collider Accelerator Department Brookhaven National Laboratory

U.S. Department of Energy

USDOE Office of Science (SC)

Notice: This technical note has been authored by employees of Brookhaven Science Associates, LLC under Contract No.DE-AC02-98CH10886 with the U.S. Department of Energy. The publisher by accepting the technical note for publication acknowledges that the United States Government retains a non-exclusive, paid-up, irrevocable, world-wide license to publish or reproduce the published form of this technical note, or allow others to do so, for United States Government purposes.

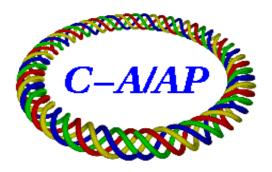
DISCLAIMER

This report was prepared as an account of work sponsored by an agency of the United States Government. Neither the United States Government nor any agency thereof, nor any of their employees, nor any of their contractors, subcontractors, or their employees, makes any warranty, express or implied, or assumes any legal liability or responsibility for the accuracy, completeness, or any third party's use or the results of such use of any information, apparatus, product, or process disclosed, or represents that its use would not infringe privately owned rights. Reference herein to any specific commercial product, process, or service by trade name, trademark, manufacturer, or otherwise, does not necessarily constitute or imply its endorsement, recommendation, or favoring by the United States Government or any agency thereof or its contractors or subcontractors. The views and opinions of authors expressed herein do not necessarily state or reflect those of the United States Government or any agency thereof.

C-A/AP/#276 May 2007

Modeling RHIC Linear Chromaticity with Sextupole Components in the Arc Main Dipoles

Y. Luo, A. Jain, W. Fischer, S. Tepikian, D. Trbojevic



Collider-Accelerator Department Brookhaven National Laboratory Upton, NY 11973

Modeling RHIC linear chromaticity with sextupole components in the arc main dipoles

Y. Luo, A. Jain, W. Fischer, S. Tepikian, and D. Trbojevic Brookhaven National Laboratory, Upton, NY 11973, USA

The sextupole components in the arc main dipoles complicate predications of the linear chromaticities in the Relativistic Heavy Ion Collider (RHIC). In this article, the measured linear chromaticity splits are modeled with the sextupole components in the arc main dipoles. The values for the equivalent average sextupole strength $(K_2L)_{dipole,mean}$ in the main dipoles are derived with an offline optics model at Blue ring injection, Blue ring store, and Yellow ring injection. The findings are compared to the b_2 estimates from the bench measurements of the magnetic field. Reasons for the discrepancy between them are suggested.

1 Introduction

It is difficult to predict the linear chromaticities, Q's, for the RHIC rings with the online optics models. The major contribution to the discrepancy between the Q' measurements and their predictions is the sextupole components in the arc main dipoles. Furthermore, at the injection energy, the sextupole component in the arc main dipole varies because of the persistent current effect [1].

Out of 288 arc main dipoles in the Blue and Yellow rings, only about 20% were bench measured in the superconducting state before going into the RHIC's tunnel. In the online optics model, the strengths for the sextupole components in the arc main dipoles are partly extracted from this limited number of bench measurements, and partly from warm-cold correlations and interpolations.

Tab. 1 shows one example of measured and predicted Q's taken at the Blue ring injection [2]. With the 2004 Au run online optics model, the error in predicating linear chromaticity is about ∓ 14 units, while with the updated 2007 Au run optics model, the error in predication is about ∓ 7 units. The two online models differ only in the strength settings of the sextupole components in arc main dipoles.

	Measurement	Online Model	Online Model
		Au04 Version	Au07 Version
Horizontal tune, Q_x	28.224	28.253	28.243
Vertical tune, Q_y	29.238	28.230	28.241
Linear horizontal chromaticity, Q'_x	-8.1	-26.5	-15.0
Linear vertical chromaticity, Q'_y	-7.1	7.0	-0.08

Table 1: Example of measurements and predictions of Q's at the Blue ring injection.

2 Beam-based measurement and modeling

2.1 Modeling procedure

In the following, we assume that the differences in the measured Q's and their predictions from the bare optics are solely due to the sextupole components in the arc main dipoles. In the bare optics, there is no sextupole component in the arc main dipoles. The contributions from the interaction regions are ignored, as well as the optical deviations.

In our following offline optics model, we artificially split the arc main dipoles into two halves and insert one sextupole multipole between. Considering there are 144 arc main dipoles in each RHIC ring, it is accurate to use the average integrated strength $(K_2L)_{dipole,mean}$ of these sextupole multipoles to model the Q' measurements. In the following modeling, all the sextupole multipoles in the arc main dipole centers have the same strength, $(K_2L)_{dipole,mean}$.

In each case, with the offline optics model, we first reproduce the measured horizontal and vertical tunes by adjusting the main quadrupole strengths. Then, with the real strengths of chromatic sextupoles, we alter $(K_2L)_{dipole,mean}$ in the offline model to minimize χ ,

$$\chi = |Q'_{x,meas.} - Q'_{x,model,b2}| + |Q'_{y,meas.} - Q'_{y,model,b2}|.$$
(1)

In total, there are 24 chromatic sextupole families in each RHIC ring. They can be sorted into 2 families, which only allows the linear chromaticity correction, or into 8 families for the nonlinear chromaticity correction. For simplicity, in the following study, we use 2 chromatic sextupole families, SF and SD, to set $Q'_{x,y}$.

2.2 At the Blue ring injection

At the 23 GeV Au injection, the β^* s at the crossing points are 10m. The natural linear chromaticities are about -45. Tab. 2 shows two cases of $Q'_{x,y}$ measurements and modeling at the Blue ring injection. Comparing the Q' predictions from the bare optics which has no sextupole components (b_2 s) in arc main dipoles, we have

$$Q'_{x,y,meas,} \approx Q'_{x,y,model,no-b2} \mp 20.0, for \ Case \ 1, \tag{2}$$

$$Q'_{x,y,meas.} \approx Q'_{x,y,model,no-b2} \mp 17.6, for \ Case \ 2.$$

$$(3)$$

Then, adjusting $(K_2L)_{dipole,mean}$ to minimize χ , for Case 1, we have $(K_2L)_{dipole,mean} \approx -0.054 \text{m}^{-2}$, and for Case 2, this value is about -0.047m^{-2} .

2.3 At the Yellow ring injection

Tab. 3 shows two cases of $Q'_{x,y}$ measurements and modeling at the Yellow ring injection, wherein

$$Q'_{x,y,meas.} \approx Q'_{x,y,model,no-b2} \mp 20.1, for \ Case \ 3, \tag{4}$$

$$Q'_{x,y,meas} \approx Q'_{x,y,model,no-b2} \mp 19.8, for \quad Case \ 4.$$

Again, adjusting $(K_2L)_{dipole,mean}$ to minimize χ , we obtain $(K_2L)_{dipole,mean} \approx -0.055 \text{m}^{-2}$ for both cases. The values of $(K_2L)_{dipole,mean}$ from the Blue and Yellow injection beam-based Q' modeling are very close.

2.4 At the Blue ring store

At 250GeV Au store, the β^* s are 0.85m at IP6 and IP8, 5m at IP10, IP2, and IP4, and 7m at IP12. The natural linear chromaticities are about -83. Tab. 4 shows two cases of $Q'_{x,y}$ measurements and modeling, and we have

$$Q'_{x,y,meas.} \approx Q'_{x,y,model,no-b2} \pm 3.5, for \quad Case \ 5.$$
(6)

$$Q'_{x,y,meas.} \approx Q'_{x,y,model,no-b2} \pm 3.1, for \quad Case \ 6.$$

$$\tag{7}$$

Manipulating $(K_2L)_{dipole,mean}$ to minimize χ , we derive $(K_2L)_{dipole,mean} \approx 0.0095 \text{m}^{-2}$, which is about six times smaller than that from the injection, and has a different sign.

2.5 At the Yellow ring store

Tab. 5 shows the Q's measurements and modeling at the Yellow ring store. According to this table, both $Q'_{x,y,meas.}$ are larger than their predictions without sextupole components in the arc main dipoles. This behavior is unlike that observed at the Blue ring injection and store, and Yellow ring at injection, where the $Q'_{x,y}$ splits are observed, and furthermore, can be modeled with sextupole components in arc main dipoles.

Since the values for $(K_2L)_{dipole,mean}$ derived from the Blue and Yellow injections are very close, we choose to adopt $(K_2L)_{dipole,mean}$ obtained from the Blue store to model Q' measurements at the Yellow store. Then, we obtain an empirical equation for the linear chromaticities at the Yellow store,

$$Q'_{x,y,meas.} \approx Q'_{x,y,model,b2} + 6. \tag{8}$$

Here, $(K_2L)_{dipole,mean} = 0.0095 \text{ m}^{-2}$ is used. The source of the 6 unit shift-up in both horizontal and vertical linear chromaticities is unknown. They may be due to various sources. In this Au 2007 run, the IR nonlinear corrections are not applied.

Case 1:	
Tunes (Q_x, Q_y)	(28.224, 29.238)
Chromic sextupole strengths	SF: $0.1769m^{-3}$, SD: $-0.1606m^{-3}$
(Q'_x, Q'_y) Measured	(-8.1,-7.1)
(Q'_x, Q'_y) from modeling:	
with $(K_2L)_{dipole,mean} = 0m^{-2}$	(11.7, -27.4)
with $(K_2 L)_{dipole,mean} = -0.054 \text{m}^{-2}$	(-8.4, -8.8)
Case 2:	
Tunes (Q_x, Q_y)	(28.230, 29.222)
Chromic sextupole strengths	SF: $0.1896m^{-3}$, SD: $-0.1968m^{-3}$
(Q'_x, Q'_y) Measured	(-2.9, -3.6)
(Q'_x, Q'_y) from modeling:	
with $(K_2L)_{dipole,mean} = 0 \text{m}^{-2}$	(14.3, -21.4)
with $(K_2 L)_{dipole,mean} = -0.047 \text{m}^{-2}$	(-3.2, -5.3)

Table 2: Blue injection: Linear chromaticity measurements and modeling.

Table 3: Yellow injection: Linear chromaticity measurements and modeling.

Case 3:	
Tunes (Q_x, Q_y)	(28.231, 29.217)
Chromic sextupole strengths	SF: $0.1769m^{-3}$, SD: $-0.1606m^{-3}$
(Q'_x, Q'_y) Measured	(-6.4, -6.9)
(Q'_x, Q'_y) from modeling:	
with $(K_2L)_{dipole,mean} = 0 \mathrm{m}^{-2}$	(13.5, -27.3)
with $(K_2 L)_{dipole,mean} = -0.055 \text{m}^{-2}$	(-6.3, -8.8)
Case 4:	
Tunes (Q_x, Q_y)	(28.230, 29.216)
Chromic sextupole strengths	SF: $0.1876m^{-3}$, SD: $-0.1737m^{-3}$
(Q'_x, Q'_y) Measured	(-4.1, -5.2)
(Q'_x, Q'_y) from modeling:	
with $(K_2L)_{dipole,mean} = 0 \text{m}^{-2}$	(15.5, -25.26)
with $(K_2L)_{dipole,mean} = -0.055 \mathrm{m}^{-2}$	(-4.0, -7.1)

2.6 Summary of beam-based modeling

From these beam-based Q' measurements and modeling, there are about 20 unit Q' split observed at the RHIC injection. If we assume they are solely contributed by the sextupole components in the arc main dipoles, we obtain the average strength of these sextupole multipoles in the arc main dipoles $(K_2L)_{dipole,mean} \approx -0.0505 \text{m}^{-2}$.

At the Blue ring store, there are about 3.5 unit Q' split in the measured $Q'_{x,y,meas.}$, giving $(K_2L)_{dipole,mean} \approx 0.0095 \text{m}^{-2}$. The $(K_2L)_{dipole,mean}$ derived at the Blue store is about 6 times smaller than that from the injection. Also, the sign of $(K_2L)_{dipole,mean}$ at the Blue store is opposite to that at the Blue injection.

For the Yellow ring store, we couldn't model the measured chromaticity shifts with sextupole multipoles in the center of arc main dipoles because both measured chromaticities $Q'_{x,y}$ are higher than their predictions from the bare optics. If we adopt the value of $(K_2L)_{dipole,mean}$ obtained from the modeling at the Blue ring store, we get about +6 unit shift-up for both horizontal and vertical chromaticities. We do not know the reason underlying this.

3 Comparing to bench measurements of magnetic field

In this section, we compare the sextupole components in the arc main dipoles from the above beam-based modeling with those from the bench measurements of magnetic field.

Case 5:	
Tunes (Q_x, Q_y)	(28.228, 29.215)
Chromic sextupole strengths	SF: $0.3310m^{-3}$, SD: -0.6575^{-3}
(Q'_x, Q'_y) Measured	(4.0, 4.3)
(Q'_x, Q'_y) from modeling:	
with $(K_2L)_{dipole,mean} = 0 \text{m}^{-2}$	(0.8, 8.2)
with $(K_2 L)_{dipole,mean} = 0.0095 \text{m}^{-2}$	(4.0, 5.1)
Case 6:	
Tunes (Q_x, Q_y)	(28.232, 29.227)
Chromic sextupole strengths	SF: $0.3202m^{-3}$, SD: $-0.6348m^{-3}$
(Q'_x, Q'_y) Measured	(1.5, 1.6)
(Q'_x, Q'_y) from modeling:	
with $(K_2L)_{dipole,mean} = 0 \text{m}^{-2}$	(-1.2, 5.1)
with $(K_2L)_{dipole,mean} = 0.0095 \text{m}^{-2}$	(1.9, 2.0)

Table 4: Blue store: Linear chromaticity measurements and modeling.

Table 5: Yellow store: linear chromaticity measurement and modeling.

Case 7:	
Tunes (Q_x, Q_y)	(28.232, 29.218)
Chromic sextupole strengths	SF: $0.2877m^{-3}$, SD: -0.5723^{-3}
(Q'_x, Q'_y) Measured	(2.3, 1.7)
(Q'_x, Q'_y) from modeling:	
with $(K_2L)_{dipole,mean} = 0 \mathrm{m}^{-2}$	(-7.7, -1.2)
with $(K_2 L)_{dipole,mean} = 0.0095 \text{m}^{-2}$	(-4.5, -4.2)
Case 8:	
Tunes (Q_x, Q_y)	(28.236, 29.226)
Chromic sextupole strengths	SF: $0.2829m^{-3}$, SD: $-0.5583m^{-3}$
(Q'_x, Q'_y) Measured	(1.1, 0.14)
(Q'_x, Q'_y) from modeling:	
with $(K_2L)_{dipole,mean} = 0 \mathrm{m}^{-2}$	(-8.7, -3.4)
with $(K_2L)_{dipole,mean} = 0.0095 \mathrm{m}^{-2}$	(-5.5, -6.5)

3.1 Conventions in magnetic field measurement

In the convention of the RHIC magnet field measurement, the integrated magnet field multipoles are [3, 4]

$$(B_yL) + i(B_xL) = [B(R_{ref})L] \left[10^{-4} \sum_{n=0}^{N_{max}} (b_n + ia_n) \frac{(x+iy)^n}{R_{ref}^n} \right].$$
(9)

Here, b_n and a_n , n = 0, 1, 2, ..., are the measured normal and skew multipole field coefficients. n = 0 represents the dipole field. $B(R_{ref})$ is the main field at radius $R_{ref} = 25$ mm for the arc dipoles. L is the magnet's length. 10^{-4} in Eq. (8) is used for normalization, for example, for the arc main dipole magnets, $b_0 = 10^4$.

According to Eq. (8), for an arc main dipole magnet, its normal sextupole component is

$$[(B_yL) + i(B_xL)]_{sextupole} = [B(R_{ref})L] \times 10^{-4} \times b_2 \times \frac{(x+iy)^2}{R_{ref}^2}.$$
 (10)

Then, the sextupole's integrated strength is

$$(K_2L) = \frac{1}{(B\rho)} \frac{\partial^2 B_y}{\partial x^2} \times L$$

= $\frac{[B(R_{ref})L]}{(B\rho)} \times 10^{-4} \times b_2 \times \frac{2}{R_{ref}^2}$ (11)
= $\Delta \theta_{bending} \times 10^{-4} \times b_2 \times \frac{2}{R_{ref}^2}.$

Here, $(B\rho)$ is the magnet rigidity, and $\Delta\theta_{bending}$ is the horizontal bending angle given by one arc main dipole. For the RHIC arc main dipole, L = 9.440656m, $\Delta\theta_{bending} = 0.038924$ rad, then we have

$$(K_2L) = 1.245 \times 10^{-2} \times b_2 \ \mathrm{m}^{-2}.$$
 (12)

In Eq. (11), we assumed b_2 is constant from end to end in the dipole. Eq. (11) is applicable at the injection and the store.

3.2 Results of bench measurements of magnetic field

About 20% of the RHIC arc main dipoles were bench measured in the superconducting state before going into the RHIC tunnel. Integrated field harmonics were measured in these magnets at three currents, 600A, 1450A and 5000A. Field harmonics also were measured at a central 1m-long section at about 35 currents, from 50A to 6000A. Furthermore, 100% of the magnets were measured warm at a current of 30A.

In the RHIC 2007 Au run, the main dipole currents at the injection and the store are 473A and 5041A, respectively. First, correlations between warm data and cold data are derived as a function of current, based on measurements at the same 1m-long section of each magnet. The correlation is interpolated for the actual injection and store currents. This warm-cold shift then is applied to the mean values of body harmonics measured warm in 100% of the arc main dipoles. This gives an estimate of the mean body b_2 at the current of interest for 100% of the magnets.

To obtain the integral b_2 values, the contributions from the magnet ends must be added. Warm-cold correlation for the ends are available only at 660A, 1450A and 5000A. However, the current dependence of this correlation for ends is rather weak, and magnet-to-magnet variation is small. Hence, we use the mean values measured at 660A and 5000A for the end harmonics.

Tab. 7 shows the b_2 s for the RHIC arc main dipoles predicted from the bench measurements. For the body, b_2 is assumed constant from end to end. For the lead and return ends, the b_2 s are normalized by the dipole's length. For example, at the injection, the integrated b_2 s for lead and return ends are $2.0 \times L$ and $0.42 \times L$, respectively.

Table 6: b_2 estimates from the bench measurements of magnetic field.

Dipole current (A)	$b_2(\text{ body })$	b_2 (lead end)	b_2 (return end)	b_2 (total)
473 (at injection)	-7.81	2.00	0.42	-5.39
5041 (at store)	-2.81	2.37	0.64	0.20

3.3 Comparing to $(K_2L)_{dipole,mean}$ from Q' modeling

Based on the linear chromaticity measurements, the linear chromaticity split is about 20 units at injection and 3.5 units at the store. With the offline model, the tune splits can be reproduced with sextupole multipoles in the centers of arc main dipoles. The averaged strengths for these sextupole multipoles are modeled about $-0.0505m^{-2}$ at injection, and about $0.0095m^{-2}$ at the store. From Eq. (8), they are equivalent to -4.06 and 0.76 in b_2 units at injection and store, respectively.

With this offline optics model, numerically, we have

$$|\Delta Q'_{x,y,inj.}| \approx \frac{20}{0.0505} \times (K_2 L)_{dipole,mean} = 396 \ (K_2 L)_{dipole,mean},\tag{13}$$

or,

$$|\Delta Q'_{x,y,inj.}| \approx \frac{20}{4.06} \times b_2 \approx 4.9b_2.$$
 (14)

At the Blue store, we have

$$|\Delta Q'_{x,y,store}| \approx \frac{3.5}{0.0095} \times (K_2 L)_{dipole,mean} = 368 \ (K_2 L)_{dipole,mean},\tag{15}$$

or,

$$|\Delta Q'_{x,y,store}| \approx \frac{3.5}{0.76} \times b_2 \approx 4.6b_2. \tag{16}$$

From Tab. 7, the total b_2 from simply summing up these values from the body, lead and return ends are about -5.39 units at injection, and about 0.20 units at the store. The differences from that from the beam-based modeling are about 1.33 and 0.56 units at the injection and the store, respectively. According to Eqs. (13) and (15), the differences give about 6.5 and 2.6 Q' splits at injection and store, respectively.

3.4 Validity of the offline model

In the above beam-based Q' modeling, we assumed the Q' splits are solely due to the sextupole components in the arc main dipoles. And with the offline model with sextupole multipoles in the centers of arc main dipoles, the Q' splits were reproduced. The linear chromaticities can be predicted very well with $(K_2L)_{dipole,mean}$ at the Blue ring store, with less than 1 unit error in predication.

In fact, to yield the same amount of shift in horizontal and vertical linear chromaticity from the sextupole multipoles in the centers of the arc main dipoles, the β_x and β_y at the center of the arc main dipoles should be equal, or comparable. From the bare optics model, at the center of the arc main dipole,

$$\frac{\beta_x}{\beta_y} \approx \frac{23.0}{21.8} \approx 1.06,\tag{17}$$

which is close to 1.

Strictly, the shifts in linear chromaticities from the sextupole components in the arc main dipoles are

$$\Delta Q'_x = -\frac{N_{dipole}}{4\pi} < K_2 D_x \beta_x >_{dipole} L, \tag{18}$$

$$\Delta Q'_y = \frac{N_{dipole}}{4\pi} < K_2 D_x \beta_y >_{dipole} L.$$
(19)

 $N_{dipole} = 144$ is the number of the arc main dipoles. Assuming K_2 is constant from end to end in the dipole,

$$\Delta Q'_x = -\frac{N_{dipole}}{4\pi} (K_2 L) < D_x \beta_x >_{dipole, body}, \tag{20}$$

$$\Delta Q'_y = \frac{N_{dipole}}{4\pi} (K_2 L) < D_x \beta_y >_{dipole, body}.$$
⁽²¹⁾

At the injection, the ratio of the averaged $\langle D_x \beta_x \rangle_{dipole, body}$ and $\langle D_x \beta_y \rangle_{dipole, body}$ is

$$\frac{\langle D_x \beta_x \rangle_{dipole, body}}{\langle D_y \beta_y \rangle_{dipole, body}} \approx \frac{33.3}{29.2} \approx 1.14,$$
(22)

so giving almost same Q' shifts in the horizontal and vertical linear chromaticities.

Substituting $\langle D_x \beta_x \rangle_{dipole, body}$ and $\langle D_y \beta_y \rangle_{dipole, body}$ into Eqs. (19) and (20), we obtain

$$|\Delta Q'_{x,y,inj.}| \approx 358 \ (K_2 L)_{dipole,mean},\tag{23}$$

or, in b_2 ,

$$|\Delta Q'_{x,y,inj.}| \approx 4.4 \ b_2. \tag{24}$$

Eqs. (22) and (23) are comparable to Eqs. (12) and (13) that from the numerical modeling, respectively.

In summary, if we assume that the sextupole component is constant in the dipole, the measured Q' splits can be equivalently modeled with the sextupole multipoles in the centers of arc main dipoles.

3.5 Effects of the dipole ends

If the contributions to Q's from b_2 s at dipole ends cannot be ignored, and/or $D_x\beta_x$ and $D_x\beta_y$ vary greatly from end to end, the contributions to Q's from the dipole body and the two ends must be evaluated separately. Tab. 8 lists the optics parameters from the bare optics model and the integrated b_2 s from bench measurements.

It is apparent from Tab. 8 that, at the injection, the contribution to Q's from the return end is smaller than that from the body and the lead end. The contribution to Q's from the lead end is about one third of that from the body. Further, according to Tab. 8, the signs of the b_2 s for the body and the lead end are opposite.

The RHIC arc main dipoles in each ring were installed with all the lead ends pointing to the same direction. Considering asymmetric β functions on both sides of the IPs, averaged along the whole ring, the contributions from lead or return ends to the horizontal and vertical linear chromaticities should be approximately same. Hence, their contributions to Q's from the lead and return ends also should be equivalently modeled with the sextupole multipoles in the centers of arc main dipoles.

Table 7: At injection: Optics parameters and b_{2} s measured at the dipole ends and averaged along the dipole body at injection

Parameters	$D_x \beta_x$	$D_x \beta_y$	$(D_x\beta_x)/(D_x\beta_y)$	Integrated b_2
one dipole end	50.3	20.6	2.4:1	4.0 (return)
the other dipole end	13.2	38.5	1:2.9	18.9 (lead)
averaged in the dipole body	33.3	29.2	1.1	-73.7

At the store, the b_2 s in the magnet's body and lead end almost cancel out each other. The total b_2 is much smaller than that at the injection.

3.6 Updating the offline model

Here, we update our offline optics model by appending two extra sextupole multipoles to both ends of each arc main dipole to evaluate the Q' contributions from the arc ends. At injection, according Eq. (11) and Tab. 7, from the b_2 estimates from magnet bench measurements, $(K_2L)_{dipole, bench, body} = -0.097 \text{ m}^{-1}$, $(K_2L)_{dipole, bench, lead} = 0.025 \text{ m}^{-1}$, and $(K_2L)_{dipole, bench, return} = 0.005 \text{ m}^{-1}$.

Tab. 9 shows the calculated Q' shifts with the updated offline model, for Case 1. The b_2 s estimated from the bench measurements give about ± 26.4 units of $Q'_{x,y}$ split. From the beam measurement, the $Q'_{x,y}$ split is $\sim \pm 20$ units. 6 units in the Q' split is equivalent to 1.2 unit change in b_2 , which is in agreement with $\Delta b_2 \approx 1.3$ from the rough estimate based on the earlier offline model in section 3.3.

Table 8: Blue injection (Case 1): Linear chromaticity measurement and modeling with the updated offline model.

Simulation condition	(Q'_x, Q'_y) from model	$(\Delta Q'_x, \Delta Q'_y)$
without (K_2L) in arc main dipoles	(11.6, -27.4)	-
only with $(K_2L)_{dipole, bench, body}$	(-24.1, 6.2)	(-35.7, 33.6)
only with $(K_2L)_{dipole, bench, lead}$	(23.3, -36.3)	(11.7, -8.9)
only with $(K_2L)_{dipole, bench, return}$	(9.3, -25.6)	(-2.3, 2.1)
with all above	(-14.7, -0.9)	(-26.3, 26.5)

3.7 Summary of b_2 comparison

In this section, we compared the mean sextupole component strength $(K_2L)_{dipole,mean}$ from the beam-based Q' modeling to the b_2 estimates from the bench measurements. The discrepancies are about 1.3 unit in b_2 at the injection, and about 0.56 unit in b_2 at the store, even with the updated offline optics model. They yield about 6 and 2.6 Q' splits at the injection and the store, respectively.

There are several possible reasons for the discrepancies in the above comparison. For example, at injection, the persistent current effect is not included in the b_2 estimates. According to Ref. [5], this effect easily

accounts for a 1.3 unit change in b_2 at injection. Similarly, for the store, out of the discrepancy of 0.56 units in b_2 , about 0.3 units could come from the uncertainty in the warm-cold correlation. Besides the errors in b_2 estimates, the deviations in the beam optics and other unknown sextupole components, for example, those in the interaction regions, also could contribute to the discrepancies.

4 Conclusion

The measured linear chromaticity splits are modeled with the sextupole components in the arc main dipoles. The equivalent $(K_2L)_{dipole,mean}$ s for the sextupole multipoles artificially placed in the center of arc main dipoles are derived with the offline optics model for the Blue ring injection, Blue ring store and Yellow ring injection. They are compared to the b_2 estimates from the magnet field's bench measurements. The possible reasons for the discrepancies are discussed. With the derived $(K_2L)_{dipole,mean}$ at the Blue ring store, the linear chromaticities can be predicted with the offline model with error less than 1 unit. At the Yellow ring store, the origin of the +6 unit shift-ups in both horizontal and vertical linear chromaticities is not understood.

5 Acknowledgments

We would like to thank S. Peggs, V. Litvinenko and T. Satogata for stimulating discussions during this work. We also thank F. Pilat from the RHIC Accelerator Physics EXperiment (APEX) Committee and 2007 Au run coordinator, and A. Drees for providing us the beam time for this study.

References

- [1] W. Fischer, A. Jain and S. Tepikian, PRST-AB, 4, 041002 (2001).
- [2] N. Maltisky, private communications, 2007.
- [3] A. Jain, D. Trbojevic, F. Dell, S. Peggs, P. Wanderer and J. Wei, BNL RHIC/AP/95, August, 1996.
- [4] S. Trahern and F. Pilat, BNL RHIC/AP/99, June, 1996.
- [5] A. Jain, G. Ganetis, J. Muratore, R. Thomas and P. Wanderer, BNL Magnet Division Note 593-11 (AM-MD-294), May 10, 2000.

http://www.bnl.gov/magnets/magnet_files/Publications/FastMeasurements.pdf.